①

AD-A212 892

CMS Technical Summary Report #90-7

QUADRATIC DYNAMICAL SYSTEMS
DESCRIBING SHEAR FLOW
OF NON-NEWTONIAN FLUIDS

D. S. Malkus, J. A. Nohel,
and B. J. Plohr

UNIVERSITY
OF WISCONSIN

CENTER FOR THE
MATHEMATICAL
SCIENCES

Center for the Mathematical Sciences
University of Wisconsin—Madison
610 Walnut Street
Madison, Wisconsin 53705

August 1989

(Received August 10, 1989)

DTIC
ELECTE
SEP. 25 1989
S   B
D

89 9 25 030

UNIVERSITY OF WISCONSIN - MADISON
CENTER FOR THE MATHEMATICAL SCIENCES

QUADRATIC DYNAMICAL SYSTEMS DESCRIBING SHEAR FLOW OF NON-NEWTONIAN FLUIDS*

D. S. Malkus[1,2]

J. A. Nohel[1,3]

B. J. Plohr[1,4]

Abstract

Phase-plane techniques are used to analyze a quadratic system of ordinary differential equations that approximates a single relaxation-time system of partial differential equations used to model transient behavior of highly elastic non-Newtonian liquids in shear flow through slit dies. The latter one-dimensional model is derived from three-dimensional balance laws coupled with differential constitutive relations well-known by rheologists. The resulting initial-boundary-value problem is globally well-posed and possesses the key feature: the steady shear stress is a non-monotone function of the strain rate. Results of the global analysis of the quadratic system of ode's lead to the same qualitative features as those obtained recently by numerical simulation of the governing pde's for realistic data for polymer melts used in rheological experiments. The analytical results provide an explanation of the experimentally observed phenomenon called spurt; they also predict new phenomena discovered in the numerical simulation; these phenomena should also be observable in experiments.

---

[1]Center for the Mathematical Sciences University of Wisconsin-Madison, Madison, WI 53705.

[2]also Department of Engineering Mechanics.

[3]also Department of Mathematics.

[4]also Computer Sciences Department.

1. Introduction

The purpose of this paper is to analyze novel phenomena in dynamic shearing flows of non-Newtonian fluids that are important in polymer processing [17]. One striking phenomenon, called "spurt," was apparently first observed by Vinogradov et al. [19] in experiments concerning quasi static flow of monodispersive polyisoprenes through capillaries or equivalently through slit dies. They found that the volumetric flow rate increased dramatically at a critical stress that was independent of molecular weight. Until recently, spurt has been associated with the failure of the flowing polymer to adhere to the wall [5]. The focus of our current research is to offer an alternate explanation of spurt and related phenomena.

Understanding these phenomena has proved to be of significant physical, mathematical, and computational interest. In our recent work [12], we found that satisfactory explanation and modeling of the spurt phenomenon requires studying the full dynamics of the equations of motion and constitutive equations. The common and key feature of constitutive models that exhibit spurt and related phenomena is a non-monotonic relation between the steady shear stress and strain rate. This allows jumps in the steady strain rate to form when the driving pressure gradient exceeds a critical value; such jumps correspond to the sudden increase in volumetric flow rate observed in the experiments of Vinogradov et al. The governing systems used to model such one-dimensional flows are analyzed in [12] by numerical techniques and simulation, and in the present work by analytical methods. The systems derive from fully three-dimensional differential constitutive relations with m-relaxation times (based on work of Johnson and Segalman [8] and Oldroyd [16]). They are evolutionary, globally well posed in a sense described below, and they possess discontinuous steady states of the type mentioned above that lead to an explanation of spurt. The governing systems for shear flows through slit-dies are formulated from balance laws in Sec. 2.

Specifically, we model these flows by decomposing the total shear stress into a polymer contribution, evolving in accordance with a differential constitutive relation with a single relaxation time and a Newtonian viscosity contribution (see system (JSO) in Sec. 2.). The flows can also be modelled by a system based on a differential constitutive law with two widely spaced relaxation times (see system (JSO_2) in [13].) but no Newtonian viscosity contribution. Numerical simulation [9, 12] of transient flows at high Weissenberg (Deborah) number and very low Reynolds number using the model (JSO) exhibited spurt, shape memory, and hysteresis; furthermore, it predicted other effects, such as latency, normal stress oscillations, and molecular weight dependence of hysteresis, that should be analysed further and tested in rheological experiment.

In earlier work, Hunter and Slemrod [7] used techniques of conservation laws to study the qualitative behavior of discontinuous steady states in a simple one-dimensional viscoelastic model of rate type with viscous damping. They predicted shape memory and hysteresis effects related to spurt. A salient feature of their model is linear instability and loss of evolutionarity in a certain region of state space.

The objective of the present paper is to develop analytical techniques, the results of which verify these rather dramatic implications of numerical simulation. Based on scaling introduced in [12], appropriate for the highly elastic and very viscous polyisoprenes used in

-2-

the spurt-experiment, we are led to study the following pair of quadratic autonomous ordinary differential equations that approximates the governing system (JSO) in the relevant range of physical parameters for each fixed position in the channel:

$$\dot{\sigma} = (Z + 1)\left(\frac{\overline{T} - \sigma}{\varepsilon}\right) - \sigma \ ;$$
$$\dot{Z} = -\sigma\left(\frac{\overline{T} - \sigma}{\varepsilon}\right) - Z \ . \tag{1.1}$$

Here the dot denotes the derivative d/dt, $\overline{T}$ is a parameter that depends on the driving pressure gradient as well as position x in the channel, and $\varepsilon > 0$ is a ratio of viscosities. System (1.1) is obtained by setting $\alpha = 0$ in the momentum equation in system (JSO); this approximation is reasonable because α is at least several orders of magnitude smaller than ε. We show that steady states of system (JSO), some of which are discontinuous for non-monotone constitutive relations, correspond to to critical points of the quadratic system. We deduce the local characters of the critical points, and we prove that system (1.1) has no periodic orbits or closed separatrix cycles. Moreover, this system is endowed with a natural Lyapunov-like function with the aid of which we are able to determine the global dynamics of the approximating quadratic system completely and thus identify its globally asymptotically stable crical points (i.e. steady states) for each position x. This analysis is carried out in Sec. 3 When α, the ratio of Reynolds to Deborah numbers, is strictly positive, the stability of discontinuous steady states of system (JSO) remains to be settled. Recently, Nohel, Pego and Tzavaras [15] established such a result for simple model in which the polymer contribution to the shear stress satisfies a single differential constitutive relation: for a particular choice, their model and system (JSO) with $\alpha > 0$ have the same behavior in steady shear. Their asymptotic stability result, combined with numerical experiments and research in progress, suggest that the same result holds for the full system (JSO), at least when α is sufficiently small.

In Sec. 4..the analysis of Sec. 3. is applied to each point x in the channel, allowing us to explain spurt. shape memory, hysteresis, and other effects originally observed in the numerical simulations in terms of a continuum of phase portraits. We discuss asymptotic expansions of solutions of systems (JSO) and (JSO_2) of Ref. [13] in powers of ε that enable us to explain latency (a pseudo-steady state that precedes spurt). The asymptotic analysis also permits a more quantitative comparison of the dynamics of the two models when ε is sufficiently small. In Sec. 5., we discuss physical implications of the analysis, particularly those that suggest new experiments. In Sec. 6., we draw certain conclusions. Although the analysis in this paper applies only to the special constitutive models we have studied, we expect that the qualitative features of our results appear in a broad class of non-Newtonian fluids. Indeed. numerical simulation by Kolkka and Ierley [10] using another model with a single relaxation time and Newtonian viscosity exhibits very similar character.

2. A Johnson-Segalman-Oldroyd Model for Shear Flow

The motion of a fluid under incompressible and isothermal conditions is governed by the balance of mass and linear momentum. The response characteristics of the fluid are embodied in the constitutive relation for the stress. For viscoelastic fluids with fading memory, these relations specify the stress as a functional of the deformation history of the fluid. Many sophisticated constitutive models have been devised; see Ref. [2] for a survey. Of particular interest is a class of differential models with m-relaxation times, derived in a three-dimensional setting in Refs. [12] and [13]; these models can be regarded as a special cases of the Johnson-Segalman model [S] when the memory function is a linear combination of m-decaying exponentials with positive coefficients or of the Oldroyd differential constitutive equation [16].

Essential properties of constitutive relations are exhibited in simple planar Pciseuille shear flow. We study shear flow of a non-Newtonian fluid between parallel plates, located at $x = \pm h/2$, with the flow aligned along the y-axis, symmetric about the center line, and driven by a constant pressure gradient $\overline{f}$. We restrict attention to the simplest model of a single relaxation-time differential model that possesses steady state solutions exhibiting a non-monotone relation between the total steady shear stress and strain rate, and thereby reproduces spurt and related phenomena discussed below. The total shear stress T is decomposed into a polymer contribution and a Newtonian viscosity contribution. When restricted to one space dimension the initial-boundary value problem, in non-dimensional units with distance scaled by h, governing the flow can be written in the form (see Refs. [9, 12]):

$$\alpha v_t - \sigma_x = \varepsilon v_{xx} + \overline{f} ,$$
$$\sigma_t - (Z + 1)v_x = -\sigma , \qquad\qquad (JSO)$$
$$Z_t + \sigma v_x = -Z$$

on the interval $[-1/2, 0]$, with boundary conditions

$$v(-1/2, t) = 0 \quad \text{and} \quad v_x(0, t) = 0 \qquad\qquad (BC)$$

and initial conditions

$$v(x, 0) = v_0(x) , \quad \sigma(x, 0) = \sigma_0(x) , \quad \text{and} \quad Z(x, 0) = Z_0(x) , \, on - 1/2 \le x \le 0; \quad (IC)$$

symmetry of the flow and compatibility with the boundary conditions requires that $v_0(-1/2) = 0$, $v_0'(0) = 0$ and $\sigma_0(0) = 0$.

The evolution of σ, the polymer contribution to the shear stress, and of Z, a quantity proportional to the normal stress difference, are governed by the second and third equations in system (JSO). As a result of scaling motivated by numerical simulation and introduced in Ref. [12], there are only three essential parameters: α is a ratio of Reynolds number to Deborah number, ε is a ratio of viscosities, and f is the constant pressure gradient.

When $\varepsilon = 0$, and $Z + 1 \ge 0$, system (JSO) is hyperbolic, with characteristics speeds $\pm[(Z + 1)/\alpha]^{1/2}$ and 0. Moreover, for smooth intial data in the hyperbolic region and compatible with the boundary conditions, techniques in [18] can be used to establish

global well-posedness (in terms of classical solutions) if the data are small, and finite-time blow-up of classical solutions if the data are large. If $\varepsilon > 0$, system (JSO) for any smooth or piece-wise smooth data; indeed, general theory developed in [15] (see Sec. 3 and particularly Appendix A) yields global existence of classical solutions for smooth initial data of arbitrary size, and also existence of almost classical, strong solutions with discontinuities in the initial velocity gradient and in stress components; the latter result allows one to prescribe discontinuous initial data of the same type as the discontinuous steady states studied in this paper.

The steady-state solutions of system (JSO) play an important role in our discussion. Such a solution, denoted by $\overline{v}$, $\overline{\sigma}$, and $\overline{Z}$, can be described as follows. The stress components $\overline{\sigma}$ and $\overline{Z}$ are related to the strain rate $\overline{v}_x$ through the relations

$$\overline{\sigma} = \frac{\overline{v}_x}{1 + \overline{v}_x^2} \,, \quad \overline{Z} + 1 = \frac{1}{1 + \overline{v}_x^2} \,. \tag{2.1}$$

Therefore, the steady total shear stress $\overline{T} := \overline{\sigma} + \varepsilon \overline{v}_x$ is given by $\overline{T} = w(\overline{v}_x)$, where

$$w(s) := \frac{s}{1 + s^2} + \varepsilon s \,. \tag{2.2}$$

The properties of w, the steady-state relation between shear stress and shear strain rate, are crucial to the behavior of the flow. By symmetry, it suffices to consider $s \geq 0$. For all $\varepsilon > 0$, the function w has inflection points at $s = 0$ and $s = \sqrt{3}$. When $\varepsilon > 1/8$, the function w is strictly increasing, but when $\varepsilon < 1/8$, the function w is not monotone. Lack of monotonicity is the fundamental cause of the non-Newtonian behavior studied in this paper; hereafter we assume that $\varepsilon < 1/8$.

The graph of w is shown in Fig. 1. Specifically, w has a maximum at $s = s_M$ and a minimum at $s = s_m$, where it takes the values $\overline{T}_M := w(s_M)$ and $\overline{T}_m := w(s_m)$ respectively. As $\varepsilon \to 1/8$, the two critical points coalesce at $s = \sqrt{3}$.

The momentum equation, together with the boundary condition at the centerline, implies that the steady total shear stress satisfies $\overline{T} = -\overline{f}x$ for every $x \in [-\frac{1}{2}, 0]$. Therefore, the steady velocity gradient can be determined as a function of x by solving

$$w(\overline{v}_x) = -\overline{f}x \,. \tag{2.3}$$

Equivalently, a steady state solution $\overline{v}_x$ satisfies the cubic equation $P(\overline{v}_x) = 0$, where

$$P(s) := \varepsilon s^3 - \overline{T} s^2 + (1 + \varepsilon)s - \overline{T} \,. \tag{2.4}$$

The steady velocity profile in Fig. 2 is obtained by integrating $\overline{v}_x$ and using the boundary condition at the wall. However, because the function w is not monotone, there might be up to three distinct values of $\overline{v}_x$ that satisfy Eq. (2.3) for any particular x on the interval $[-1/2, 0]$. Consequently, $\overline{v}_x$ can suffer jump discontinuities, resulting in kinks in the velocity profile (as at the point x_* in Fig. 2). Indeed, a steady solution must contain such a jump if the total stress $\overline{T}_{\text{wall}} = \overline{f}/2$ at the wall exceeds the total stress $\overline{T}_M$ at the local maximum M in Fig. 1.

Finally, we remark that the flow problem discussed here can also be modelled by a system based on a differential constitutive law with two widely spaced relaxation times but no Newtonian viscosity contribution (see system (JSO_2) in Sec. 2. of [13]); with an appropriate choice of relevant parameters, the resulting problem exhibits the same steady states and the same characteristics as (JSO).
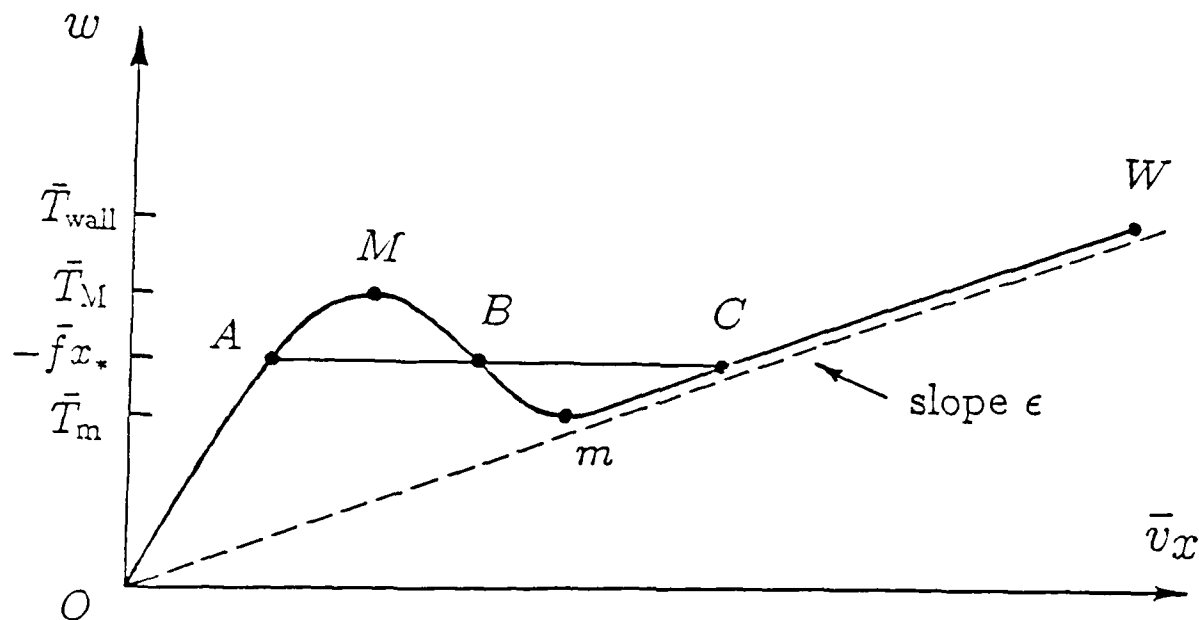
Fig. 1: Total steady shear stress $\overline{T}$ vs. shear strain rate $\overline{v}_x$ for steady flow. The case of three critical points is illustrated; other possibilities are discuss㉿ in Sec. 3.

3. Phase Plane Analysis for System (JSO) When $\alpha = 0$

When α is not zero. numerical simulation developed in [9, 11, 12] discovered striking phenomena in shear flow and suggested the analysis that follows. A great deal of information about the structure of solutions of system (JSO) can be garnered by studying a quadratic system of ordinary differential equations that approximates it in a certain parameter range. the dynamics of which is determined completely. Motivation for this approximation comes from the following observation: in experiments of Vinogradov et al. [19], α is of the order 10^{-12}; thus the term αv_t in the momentum equation of system (JSO) is negligible even when v_t is moderately large. This led us to the approximation to system (JSO) obtained when $\alpha = 0$.

When $\alpha = 0$. the momentum equation in system (JSO) can be integrated to show that the total shear stress $T := \sigma + \varepsilon v_x$ coincides with the steady value $\overline{T}(x) = -\overline{f}x$. Thus $T = \overline{T}(x)$ is a function of x only, even though σ and v_x are functions of both x and t. The remaining equations of system (JSO) yield, for each fixed x, the autonomous, quadratic,
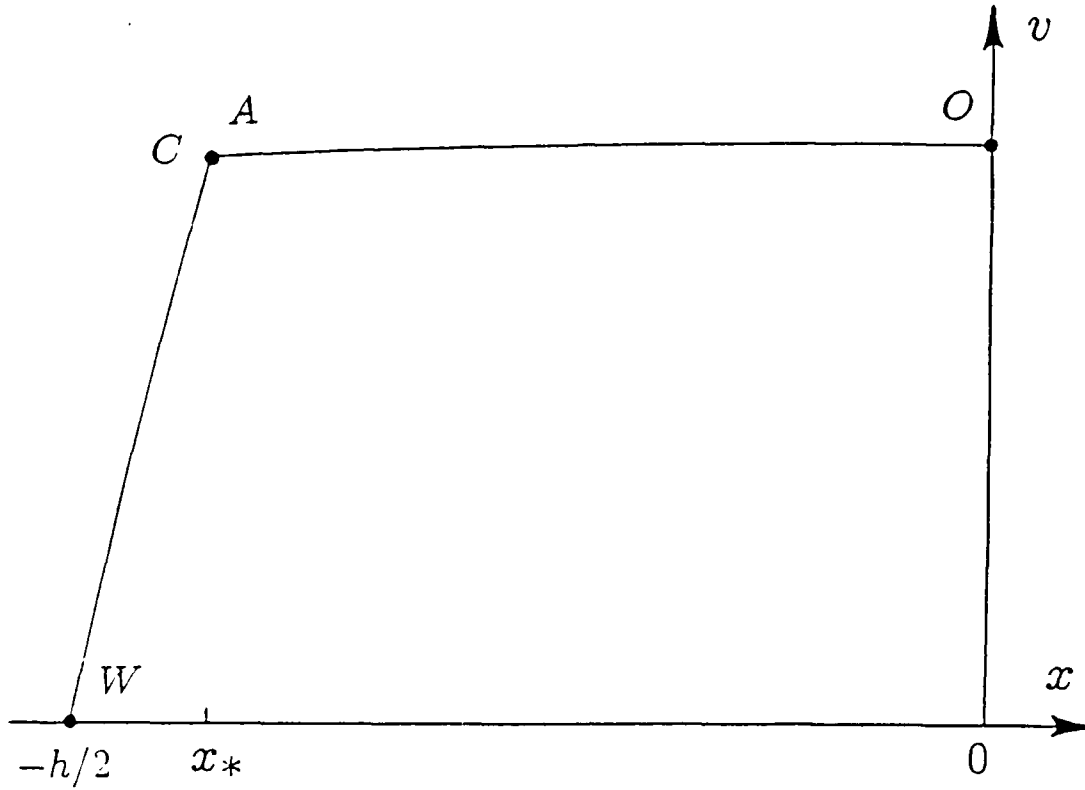
Fig. 2: Velocity profile for steady flow.

planar system of ordinary differential equations

$$\dot{\sigma} = (Z + 1)\left(\frac{\overline{T} - \sigma}{\varepsilon}\right) - \sigma \, ,$$

$$\dot{Z} = -\sigma\left(\frac{\overline{T} - \sigma}{\varepsilon}\right) - Z \, . \tag{3.1}$$

Here the dot denotes the derivative d/dt. We emphasize that for each $\overline{f}$, a different dynamical system is obtained at each x on the interval $[-1/2, 0]$ in the channel because $\overline{T} = -\overline{f}x$. By symmetry, we may focus attention on the case $\overline{T} > 0$; also recall from Sec. 2 that $\varepsilon < 1/8$: these are assumed throughout. The dynamical system (3.1) can be analyzed completely by a phase-plane analysis outlined below; the reader is referred to Sec. 3 in [13] for further details. Here we state the main results.

The critical points of system (3.1) satisfy the algebraic system

$$(Z + 1 + \varepsilon)\left(\frac{\sigma}{\overline{T}} - 1\right) + \varepsilon = 0 \, ,$$

$$\frac{\overline{T}^2}{\varepsilon}\frac{\sigma}{\overline{T}}\left(\frac{\sigma}{\overline{T}} - 1\right) - Z = 0 \, . \tag{3.2}$$

These equations define, respectively, a hyperbola and a parabola in the σ-Z plane; these curves are drawn in Fig. 3, which corresponds to the most comprehensive case of three critical points. The critical points are intersections of these curves. In particular, critical points lie in the strip $0 < \sigma < \overline{T}$.
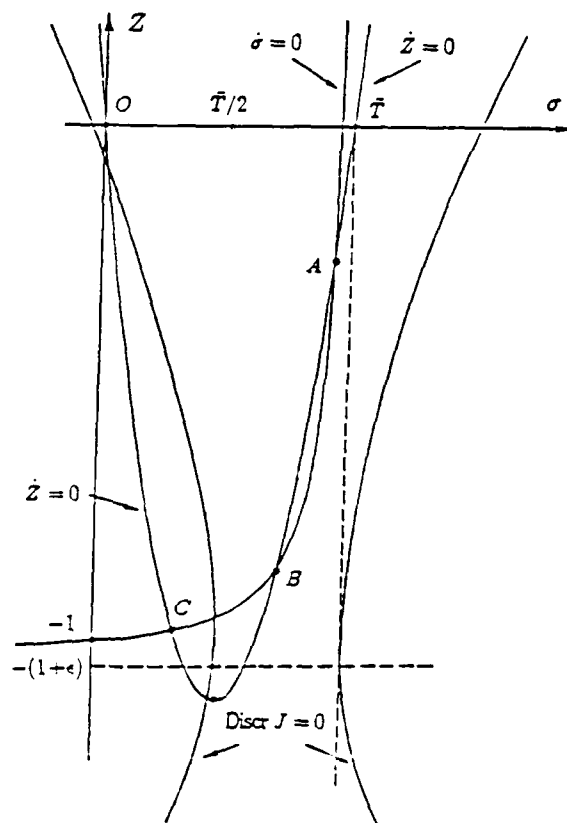

Fig. 3: The phase plane in the case of three critical points.

Eliminating Z in these equations shows that the σ-coordinates of the critical points satisfy the cubic equation $Q(\sigma/\overline{T}) = 0$, where

$$Q(\xi) := \left[\frac{\overline{T}^2}{\varepsilon} \xi(\xi - 1) + 1 + \varepsilon \right] (\xi - 1) + \varepsilon \ . \tag{3.3}$$

A straightforward calculation using Eq. (2.4) shows that

$$P(\overline{v}_x) = P\left(\frac{\overline{T} - \sigma}{\varepsilon} \right) = -\frac{\overline{T}}{\varepsilon} Q(\sigma/\overline{T}) \ . \tag{3.4}$$

Thus each critical point of the system (3.1) defines a steady-state solution of system (JSO): such a solution corresponds to a point on the steady total-stress curve (see Fig. 1) at which the total stress is $\overline{T}(x)$. Consequently, we have:

Proposition 3.1:
For each position x in the channel and for each $\varepsilon > 0$, there are three possibilities:
(1) there is a single critical point A when $\overline{T} < \overline{T}_m$;
(2) there is also a single critical point C if $\overline{T} > \overline{T}_M$;
(3) there are three critical points A, B, and C when $\overline{T}_m < \overline{T} < \overline{T}_M$.

For simplicity, we ignore the degenerate cases, where $\overline{T} = \overline{T}_M$ or $\overline{T} = \overline{T}_m$, in which two critical points coalesce.

To determine the qualitative structure of the dynamical system (3.1), we first study the nature of the critical points. The behavior of orbits near a critical point depends on the linearization of system (3.1) at this point, i.e., on the eigenvalues of the Jacobian matrix J associated with Eq. (3.1), evaluated at the critical point. To avoid solving the cubic equation $Q(\sigma/\overline{T}) = 0$, the character of the eigenvalues of J can be determined from the signs of the trace of J denoted by $\mathrm{Tr}\,J$, the determinant of J denoted by $\mathrm{Det}\,J$, and the discriminant of J denoted by $\mathrm{Discrm}\,J$ at the critical points. We omit these tedious calculations, a result of which is a useful fact: at a critical point, $\varepsilon\,\mathrm{Det}\,J = Q'(\sigma/\overline{T})$. This relation is important because Q' is positive at A and C and negative at B. To assist the reader, Fig. 3 shows the hyperbola on which $\dot{\sigma} = 0$, the parabola on which $\dot{Z} = 0$ [see Eqs. (3.2)], and the hyperbola on which $\mathrm{Discrm}\,J$ vanishes. As a result of the analysis above, we draw the following conclusions:
(1) $\mathrm{Tr}\,J < 0$ at all critical points;
(2) $\mathrm{Det}\,J > 0$ at A and C, while $\mathrm{Det}\,J < 0$ at B; and
(3) $\mathrm{Discrm}\,J > 0$ at A and B, whereas $\mathrm{Discrm}\,J$ can be of either sign at C. (For typical values of ε and $\overline{T}$, $\mathrm{Discrm}\,J < 0$ at C; in particular, $\mathrm{Discrm}\,J < 0$ if C is the only critical point. But it is possible for $\mathrm{Discrm}\,J$ to be positive if $\overline{T}$ is sufficiently close to $\overline{T}_m$.)

Standard theory of nonlinear planar dynamical systems (see, e.g., Ref. [3, Chap. 15]) now establishes the local characters of the critical points A, B, C in Proposition 3.1:

Proposition 3.2:
(1) A is an attracting node (called the classical attractor);
(2) B is a saddle point;
(3) C is either an attracting spiral point or an attracting node (called the spurt attractor).

The next task is to determine the global structure of the orbits of system (3.1). In this direction, we modify an argument suggested by A. Coppel [4] and establish the crucial result, the proof of which involves a change in the time scale and an application of Bendixson's theorem:

Proposition 3.3:
System (3.1) has neither periodic orbits nor separatrix cycles.

To understand the global qualitative behavior of orbits, we construct suitable invariant sets. In this regard, a crucial tool is that system (3.1) is endowed with the identity (3.1)

$$\frac{d}{dt}\left\{\sigma^2 + (Z+1)^2\right\} = -2\left[\sigma^2 + (Z + \tfrac{1}{2})^2 - \tfrac{1}{4}\right] . \tag{3.5}$$

Thus the function $V(\sigma, Z) := \sigma^2 + (Z+1)^2$ serves as a Lyapunov function for the dynamical system. Notice that identity (3.5) is independent of $\overline{T}$ and ε.

Let Γ denote the circle on which the right side of Eq. (3.5) vanishes, and let C_r denote the circle of radius r centered at $\sigma = 0$ and $Z = -1$, i.e. $C_r := \{(\sigma, Z) : V(\sigma, Z) = r, r > 0\}$; each C_r is a level set of V. The circles Γ and C_1 are shown in Fig. 4, which corresponds to the case of a single critical point, the spiral point C. Eq. (3.5) also implies the critical points of system (3.1) lie on Γ. If $r > 1$, Γ lies strictly inside C_r. Consequently, Eq. (3.5) shows that the dynamical system (3.1) flows inward at points along C_r. Thus the interior of C_r is a positively invariant set for each $r > 1$. Furthermore, the closed disk bounded by C_1, which is the intersection of these sets, is also positively invariant. Therefore the above argument establishes:

Proposition 3.4: *Each closed disk bounded by the circle $C_r, r \geq 1$ is a positively invariant set for the system (3.1).*

The above results combined with identification of suitable invariant sets were used to determine the global structure of the orbits of system (3.1) in the cases of one and three critical points, and to analyze the stable and unstable manifolds of the saddle point at B. These results are shown in Figs. 5 and 6 and summerized in the following result.

Proposition 3.5:
The basin of attraction of A, i.e., the set of points that flow toward A as $t \to \infty$, comprises those points on the same side of the stable manifold of B as is A; points on the other side are in the basin of attraction of C. Moreover, the arc of the circle Γ through the origin, between B and its reflection B' is contained in the basin of attraction of A. In particular, the stable manifold for B cannot cross its boundary, so that it cannot cross Γ between B and B'.

All qualitative features of the dynamics of system (3.1) (except possibly whether C is a node or a focus) carry over to one that approximates the system (JSO_2) in the case of two widely separated relaxation times (see system (4.3) in [13]).
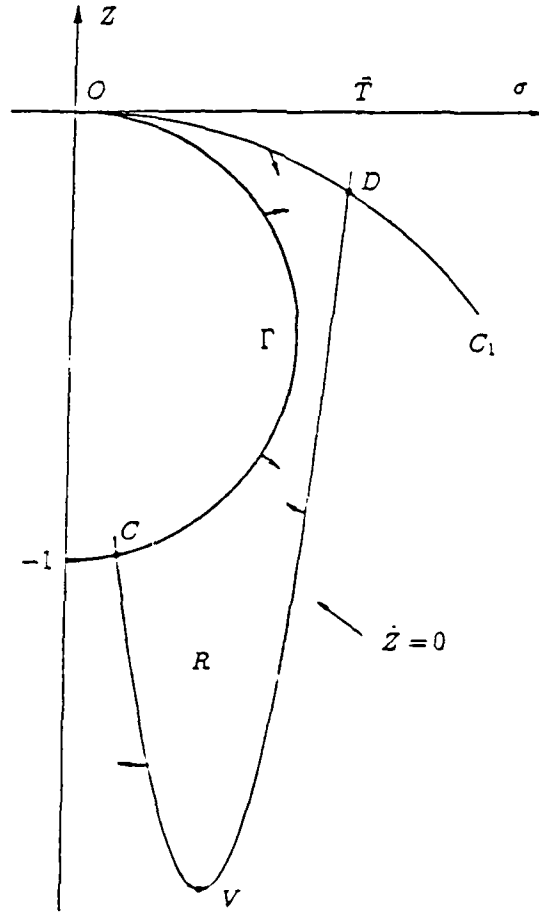
Fig. 4: The phase plane when the spurt attractor C is the only critical point.

1. Qualitative Features of (JSO) Based on Phase Plane Analysis

The discussion that follows sketches an explanation of recent numerical simulations of (JSO) described in Refs. [9, 12]. These exhibited several effects related to spurt: latency, shape memory, and hysteresis. Fig. 7 shows the result of simulating a "quasi-static" loading sequence in which the pressure gradient $\bar{f}$ is increased in small steps, allowing sufficient time between steps to achieve steady flow [9]. The loading sequence is followed by a similar quasi-static unloading sequence, in which the driving pressure gradient is decreased in steps. The initial step used zero initial data, and succeeding steps used the results of the previous step as initial data. The resulting hysteresis loop includes the shape memory predicted by Hunter and Slemrod [7] for a simpler model by a different approach. The width of the hysteresis loop at the bottom can be related directly to the molecular weight of the sample [9].

We explain spurt, shape memory, hysteresis and latency. We consider experiments of the following type: the flow is initially in a steady state corresponding to a forcing $\bar{f}_0$, and the forcing is suddenly changed to $\bar{f} = \bar{f}_0 + \Delta\bar{f}$. We call this process "loading" (resp. "unloading") if $\Delta\bar{f}$ has the same (resp. opposite) sign as $\bar{f}_0$. The initial flow can be described by specifying, for each channel position x, whether the flow is at a classical
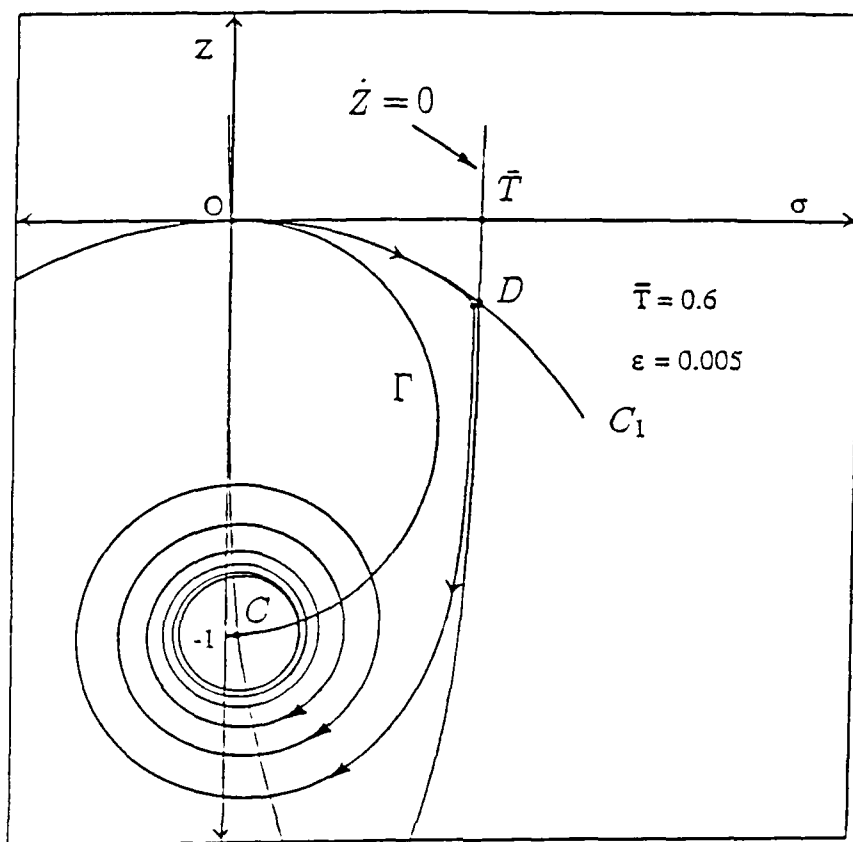
Fig. 5: The orbit through origin when the spurt attractor C is the only critical point.

attractor A (x is a "classical p int") or a spurt attractor C (x is a "spurt point") for the system (3.1) with $\overline{T} = -\overline{f}_0 x$. We shall say that any point lying on the same side of the stable manifold of B as is A lies on the "classical side"; points lying on the other side are said to be on the "spurt side." The outcome of the experiment depends on the character of the phase portrait with $\overline{T} = -\overline{f}x$. To determine this outcome, we need only decide when a classical point becomes a spurt point or vice versa.

The principle mathematical properties of the dynamical system (3.1) that determine the outcome of loading and unloading experiments are embodied in the following consequence of the phase plane analysis.

Proposition 4.1:
(1) A classical point x_0 for the initial forcing $\overline{f}_0$ lies in the domain of attraction of the classical attractor A for $\overline{f}$, provided that A exists (i.e., $|\overline{f}x| < \overline{T}_M$);
(2) A spurt point C_0 for the initial forcing $\overline{f}_0$ lies in the domain of attraction of the spurt attractor C for $\overline{f}$ unless (a) C does not exist (i.e., $|\overline{f}x| < \overline{T}_m$); or (b) C lies on the classical side of the stable manifold of the saddle point B for $\overline{f}$.

Consider starting with $\overline{f}_0 = 0$ and loading to $\overline{f} > 0$. Thus the initial state for each x
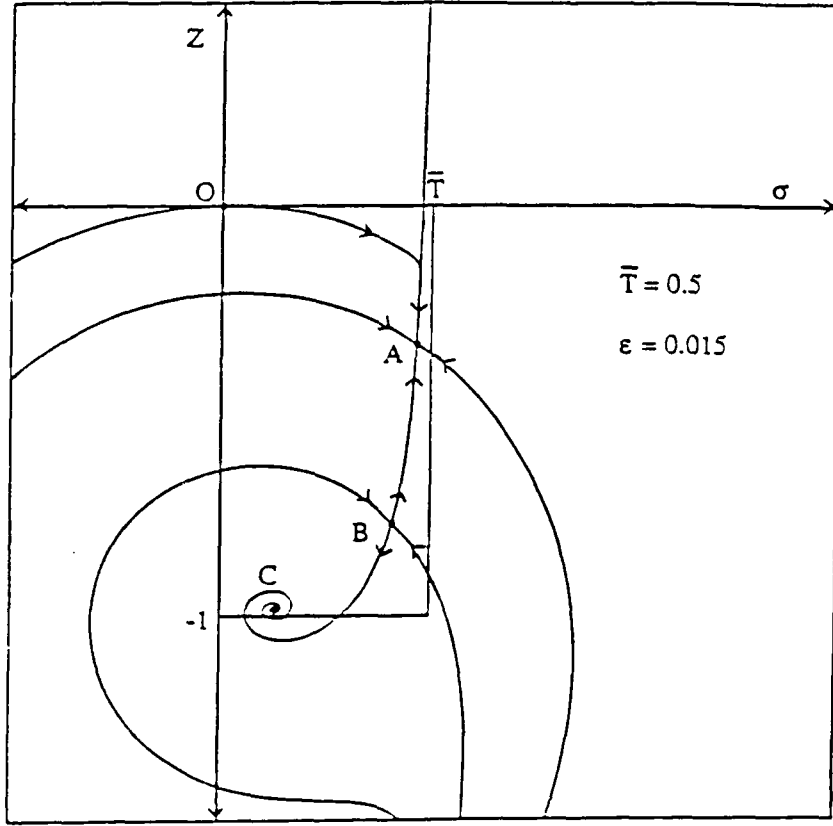
Fig. 6: Phase portrait in the case of three critical points, with C being a spiral.

lies at the origin $\sigma = 0$, $Z = 0$. Then according to 4.1(1) above, each $x \in [-1/2, 0]$ such that $\overline{f}|x| < \overline{T}_M$ is a classical point, while the x for which $\overline{f}|x| > \overline{T}_M$ are spurt points (because there is no classical attractor). Consequently, we draw two conclusions:

Proposition 4.2:
(a) *If the forcing is subcritical (i.e., $\overline{f} < \overline{f}_{crit} := 2\overline{T}_M$), the asymptotic steady flow is entirely classical.*
(b) *If the forcing is supercritical ($\overline{f} > \overline{f}_{crit}$), there is a single kink in the velocity profile (see Fig. 2), located at $x_* = -\overline{T}_M/\overline{f}$; those $x \in [-1/2, x_*)$, near the wall, are spurt points, whereas $x \in (x_*, 0]$, near the centerline, are classical.*

The solution in case (b) can be described as "top jumping" because the stress $\overline{T}_* = \overline{T}_M$ at the kink is as large as possible, and the the kink is located as close as possible to the wall.

Next, consider increasing the load from $\overline{f}_0 > 0$ to $\overline{f} > \overline{f}_0$. A point x that is classical for $\overline{f}_0$ remains classical for $\overline{f}$ unless there is no classical attractor for $\overline{T} = -\overline{f}x$, i.e., $\overline{f}|x| > \overline{T}_M$. A spurt point x for $\overline{f}_0$, on the other hand, is always a spurt point for $\overline{f}$. As a result, a point in x in the channel can change only from a classical attractor to a spurt
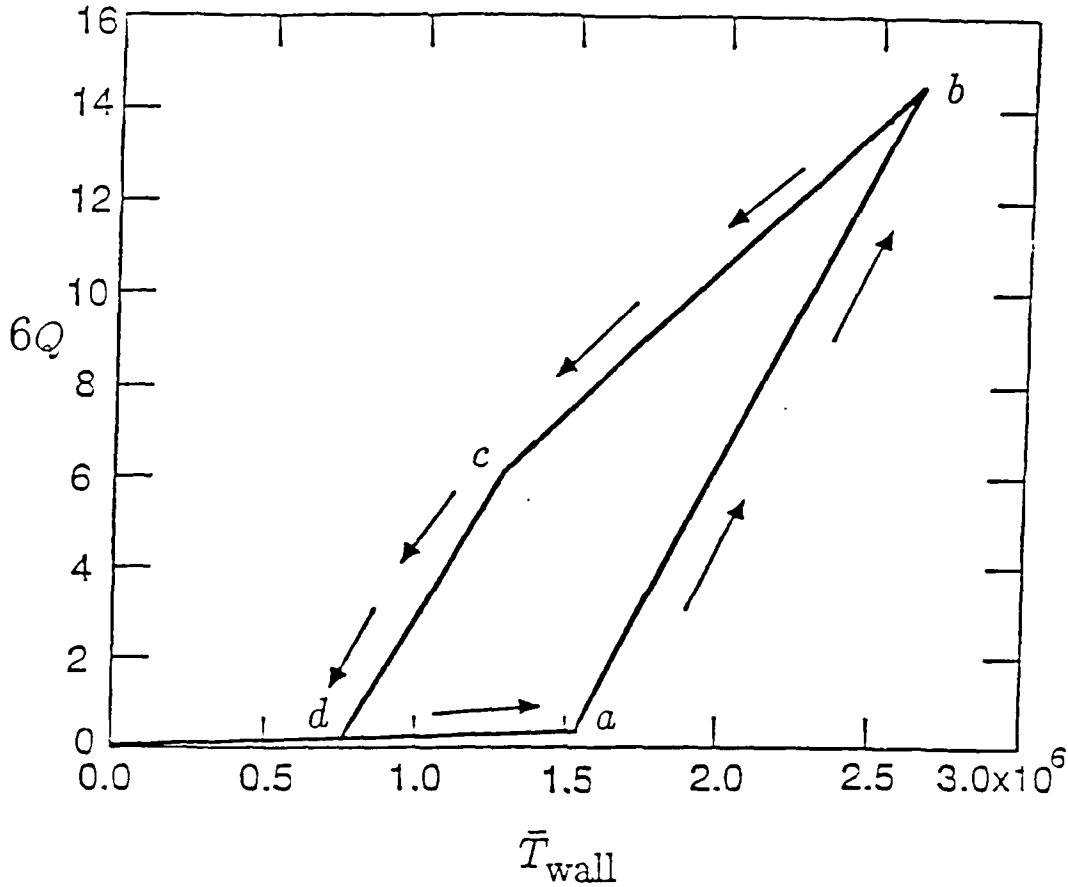
Fig. 7: Hysteresis under cyclic load: normalized throughput $6Q$ vs. wall shear stress $\overline{T}_{wall}$ [9].

attractor, and then only if $\overline{f}|x|$ exceeds $\overline{T}_M$. When $\overline{f}$ is chosen to be supercritical, loading causes the position x_* of the kink in Fig. 2 to move away from the wall, but only to the extent that it must: a single jump in strain rate occurs at $x_* = -\overline{T}_M/\overline{f}$, where the total stress is $\overline{T}_* = \overline{T}_M$. These conclusions are valid, in particular, for a quasi-static process of gradually increasing the load from $\overline{f}_0 = 0$ to $\overline{f} > \overline{f}_{crit}$.

Now consider unloading from $\overline{f}_0 > 0$ to $\overline{f} < \overline{f}_0$; assume, for the moment, that $\overline{f}$ is positive. Here, the initial steady solution need not correspond to top jumping. For this type of unloading, a point x that is classical for $\overline{f}_0$ always remains classical for $\overline{f}$: the classical attractor for $\overline{f}$ exists because $\overline{f}|x| < \overline{f}_0|x|$. By contrast, a spurt point x for $\overline{f}_0$ can become classical at $\overline{f}$. This occurs if: (a) the total stress $\overline{T} = -\overline{f}x$ falls below $\overline{T}_m$; or (b) the spurt attractor C_0 for $\overline{T} = -\overline{f}_0x$ lies on the classical side of the stable manifold of the saddle point B for $\overline{T} = -\overline{f}x$ (see Proposition 4.1(2b)).

Combining the analysis of loading and unloading leads to the following summary of quasi-static cycles and the resulting flow hysteresis.

Kinks move away from the wall under top jumping loading; they move toward the wall under bottom jumping unloading; otherwise they remain fixed. The hysteresis loop opens from the point at which unloading commences; no part of the unloading path retraces the

loading path until point d in Fig. 7.

To explain the latency effect that occurs during loading, assume that ε is small. It is readily seen that the total stress $\overline{T}_M$ at the the local maximum M is $1/2 + O(\varepsilon)$, while the local minimum m corresponds to a total stress $\overline{T}_m$ of $2\sqrt{\epsilon}\,[1 + O(\epsilon)]$. Furthermore, for x such that $\overline{T}(x) = O(1)$, $\sigma = \overline{T} + O(\varepsilon)$ at an attracting node at A, while $\sigma = O(\epsilon)$ at a spurt attractor C (which is a spiral). Consider a point along the channel for which $\overline{T}(x) > \overline{T}_M$, so that the only critical point of the system (3.1) is C, and suppose that that $\overline{T} < 1$. Then the evolution of the system exhibits three distinct phases, as indicated in Fig. 6: an initial "Newtonian" phase (O to N); an intermediate "latency" phase (N to S); and a final "spurt" phase (S to C).

The Newtonian phase occurs on a time scale of order ε, during which the system approximately follows an arc of a circle centered at $\sigma = 0$ and $Z = -1$. Having assumed that $\overline{T} < 1$, Z approaches

$$Z_N = (1 - \overline{T}^2)^{\frac{1}{2}} - 1 \tag{4.1}$$

as σ rises to the value $\overline{T}$. (If, on the other hand, $\overline{T} \geq 1$, the circular arc does not extend as far as $\overline{T}$, and σ never attains the value $\overline{T}$; rather, the system slowly spirals toward the spurt attractor. Thus the dynamical behavior does not exhibit distinct phases.)

The latency phase is characterized by having $\sigma = \overline{T} + O(\epsilon)$, so that σ is nearly constant and Z evolves approximately according to the differential equation

$$\dot{Z} = -\frac{\overline{T}^2}{Z + 1} - Z \; . \tag{4.2}$$

Therefore, the shear stress and velocity profiles closely resemble those for a steady solution with no spurt, but the solution is not truly steady because the normal stress difference Z still changes. Integrating Eq. (4.2) from $Z = Z_N$ to $Z = -1$ determines the latency period. This period becomes indefinitely long when the forcing decreases to its critical value; thus the persistence of the near-steady solution with no spurt can be very dramatic. The solution remains longest near point L where $Z = -1 + \overline{T}$. This point may be regarded as the remnant of the attracting node A and the saddle point B. Eventually the solution enters the spurt phase and tends to the critical point C. Because C is an attracting spiral, the stress oscillates between the shear and normal components while it approaches the steady state.

Asymptotic analysis carried out in Sec. 6 of [13] shows that when ε is sufficiently small, system (JSO_2) of [13] has the same asymptotic properties as system (JSO). Thus system (JSO) approximates (JSO_2) quantitatively as well as qualitatively.

5. Physical Implications

One of the widely accepted explanations of spurt and similar observations is that the presence of the wall affects the dynamics of the polymer system near the wall. Conceivably, there could be a variety of "wall effects," the most obvious is the loss of chemical bond between wall and fluid, or wall slip [5]. Perhaps the most distinguishing feature of our alternative approach is: it predicts that spurt stems from a material property of the polymer and is not related to any external interaction. The spurt layer forms at the wall in situations such as top jumping because the stresses are higher there; for the same reason, of course, is chemical bonds would break at the wall;however, our approach predicts that the layer of spurt points spreads into the interior of the channel on continued loading. Layer thickness is predicted to grow continuously in loading to a thickness that should be observable, provided secondary (two-dimensional) instabilities do not develop.

Our analysis suggests other ways in which experiments might be devised to verify the dependence of spurt on material properties: (i) produce multiple kinks with spurt layer separated from the wall, (ii) produce hysteresis in flow reversal (Fig. 9). Our model predicts circumstances under which a different path can be followed in sudden reversal of the flow than would be followed by a sequence of solutions in which the pressure gradient is reduced to zero and reloaded again (with the opposite sign) to a value of somewhat smaller magnitude. Such behavior does not seem likely to be explainable by a wall effect.

The most important and perhaps the easiest experiment to perform to verify our theory is to produce latency. Our analysis predicts long latency times for data corresponding to realistic material data: no sophisticated timing device would be required, nor would the onset of the instability be hard to identify. The increase in throughput is predicted to be so dramatic that simple visual inspection of the exit flow would probably be sufficient.

6. Conclusions

Although our analysis applies only to the special constitutive models we have studied, we expect that the qualitative features of our results appear in a broad class of non-Newtonian fluids. Our analysis has identified certain universal mathematical features in the shear flow of viscoelastic fluids described by differential constitutive relations that give rise to spurt and related phenomena. The key feature is that there are three widely separated time scales, each associated with an important non-dimensional number (α, ϵ, and 1, respectively), when scaled by the dominant relaxation time, λ^{-1}. Each of these time scales can be associated with a particular equation in system (JSO) [13]. The key to understanding the dynamics of such systems is fixing the location of the discontinuity in the strain rate induced by the non-monotone character of the steady shear stress vs. strain rate.

References

1. A. Andronov and C. Chaikin, *Theory of Oscillations*, Princeton Univ. Press, Princeton, 1949.

2. R. Bird, R. Armstrong, and O. Hassager, *Dynamics of Polymeric Liquids*, John Wiley and Sons, New York, 1987.

3. E. Coddington and N. Levinson, *Theory of Ordinary Differential Equations*, McGraw-Hill, New York, 1955.

4. A. Coppel, , 1989. private communication.

5. M. Denn, "Issues in Viscoelastic Fluid Dynamics," *Annual Reviews of Fluid Mechanics*, 1989. to appear.

6. M. Doi and S. Edwards, "Dynamics of Concentrated Polymer Systems," *J. Chem. Soc. Faraday* **74** (1978), pp. 1789–1832.

7. J. Hunter and M. Slemrod, "Viscoelastic Fluid Flow Exhibiting Hysteretic Phase Changes," *Phys. Fluids* **26** (1983), pp. 2345–2351.

8. M. Johnson and D. Segalman, "A Model for Viscoelastic Fluid Behavior which Allows Non-Affine Deformation," *J. Non-Newtonian Fluid Mech.* **2** (1977), pp. 255–270.

9. R. Kolkka, D. Malkus, M. Hansen, G. Ierley, and R. Worthing, "Spurt Phenomena of the Johnson-Segalman Fluid and Related Models," *J. Non-Newtonian Fluid Mech.* **29** (1988), pp. 303–325.

10. R. Kolkka and G. Ierley, "Spurt Phenomena for the Giesekus Viscoelastic Liquid Model," *J. Non-Newtonian Fluid Mech.*, 1989. To appear.

11. D. Malkus, J. Nohel, and B. Plohr, "Time-Dependent Shear Flow Of A Non-Newtonian Fluid," in *Conference on Current Problems in Hyberbolic Problems: RiemannProblems and Computations (Bowdoin,1988)*, ed. B. Lindquist, Amer. Math. Soc., Providence, 1989. Contemporary Mathematics, to appear.

12. D. Malkus, J. Nohel, and B. Plohr, "Dynamics of Shear Flow of a Non-Newtonian Fluid," *J. Comput. Phys.*, 1989. To appear.

13. D. Malkus, J. Nohel, and B. Plohr, "Analysis of New Phenomena In Shear Flow of Non-Newtonian Fluids," *SIAM J. Appl. Math.*, 1989. Submitted.

14. T. McLeish and R. Ball, "A Molecular Approach to the Spurt Effect in Polymer Melt Flow," *J. Polymer Sci.* **24** (1986), pp. 1735–1745.

15. J. Nohel, R. Pego, and A. Tzavaras, "Stability of Discontinuous Steady States in Shearing Motions of Non-Newtonian Fluids," *Proc. Roy. Soc. Edinburgh, Series A*, 1989. submitted.

16. J. Oldroyd, "Non-Newtonian Effects in Steady Motion of Some Idealized Elastico-Viscous Liquids," *Proc. Roy. Soc. London* **A 245** (1958), pp. 278–297.

17. J. Pearson, *Mechanics of Polymer Processing*, Elsevier Applied Science, London, 1985.

18. M. Renardy, W. Hrusa, and J. Nohel, *Mathematical Problems in Viscoelasticity*, Pitman Monographs and Surveys in Pure and Applied Mathematics, Vol. 35, Longman Scientific & Technical, Essex, England, 1987.

19. G. Vinogradov, A. Malkin, Yu. Yanovskii, E. Borisenkova, B. Yarlykov, and G. Berezhnaya, "Viscoelastic Properties and Flow of Narrow Distribution Polybutadienes and Polyisoprenes," *J. Polymer Sci., Part A-2* **10** (1972), pp. 1061–1084.

20. M. Yao and D. Malkus, "Analytical Solutions of Plane Poiseuille Flow of a Johnson-Segalman Fluid," in preparation, 1989.